J Appl Electrochem (2011) 41:161–171
DOI 10.1007/s10800-010-0220-9

ORIGINAL PAPER

Study on the wire electrochemical groove turning process

Taha Ali El-Taweel · Sherif Araby Gouda

Received: 12 January 2010 / Accepted: 21 September 2010 / Published online: 14 October 2010

Abstract In this study a copper wire is proposed as a tool electrode in electrochemical groove turning process (WECGT). The working parameters, namely, radial feed rate, wire diameter, and rotational speed are investigated to study the performance criteria via MRR, groove width, and roundness error. An experimental study is presented through performing series of designed experiments. Key features of a WECGT setup that was designed and developed incorporating several unique features are also highlighted. The experimental results are statistically analyzed and mathematically modeled through response surface methodology (RSM). The mathematical model adequacies are checked using analysis of variance (ANOVA). Furthermore, optimal combination of working parameters has been evaluated to maximize MRR and minimize roundness error. The results reveal that using wire as an electrode in electrochemical turning instead of using a profiled tool proved its powerfulness to produce circular grooves. The results also demonstrate that the groove width has greatly increased by increasing the wire diameter, while it is decreased by increasing both the radial feed rate and rotational speed. Lower roundness errors are obtained by increasing both radial feed rate and wire diameter. The optimum combination of parameters setting is: radial feed rate of 0.08 mm $min^{-}1$, wire diameter of 2.3 mm, and rotational speed of 578 rpm.

T. A. El-Taweel (✉)
Faculty of Engineering, Menoufiya University,
Shebin El-Kom, Egypt
e-mail: tahaeltaweel@yahoo.com

S. A. Gouda
High Institute of Technology, Benha University, Benha, Egypt
e-mail: sherif990@yahoo.com

Keywords Electrochemical machining · Electrochemical turning · Groove cutting · Roundness error · Response surface methodology (RSM)

1 Introduction

Electrochemical machining has become one of the most widely spread techniques of the non-traditional processes. The main problem of ECM is that of choosing the correct working parameters to attain high degree of accuracy under fine surface finish conditions. ECM is suitable for machining high alloyed materials specially those used in aerospace industry. Moreover, the process proved to be successful in dealing with complicated shapes. The cutting process in spite of being simple in its principle seems to be rather complicated due to the various parameters controlling it [1–4].

The electrochemical machining process is being extended from die sinking to turning in order to achieve a high degree of accuracy and surface finish in straight turning as well as in form turning of hard-to-machine materials having high slenderness ratio. This will simplify many turning operations in conventional and copying lathes and eliminate grinding operations. Recently, electrochemical turning has gained attention as a finishing process. By feeding a shaped tool into a rotating workpiece, axially symmetric turned parts can be manufactured. In this way large symmetric workpiece can be made with small tools. Turned parts of thin sections, which would be difficult to machine in the conventional way because of the distorting effect of the cutting forces, can also be machined by electrochemical turning [5–9]. Hofstede and Brekel [5] investigated the use of different electrode geometries (box-shaped electrode and plate electrode) in electrochemical turning process. A

theoretical analysis is presented for calculating the current density in the inter-electrode gap. In addition, they studied the roundness error of the electrochemically turned workpieces and concluded that the roundness error increases with the increase of electrode feed rate.

Dietz et al. [6] investigated the electrochemical turning process using an electrode consisting of two surface inclined to each other at an angle. They derived a theoretical model link between the minimum inter-electrode gap, feed rate, and electrode geometry. It was observed good agreement between the experimental results and the derived model. Ghabrial et al. [7] studied the electrochemical groove shaping process using shaped tube electrode. They presented a mathematical methodology which aims to transform the ECT process from an experimental technique to a mathematically based discipline. They concluded that the increase of the tool feed rate increases the groove width of cut and increases the amount of consumed current.

Wire electrochemical machining (WECM) is a cutting process in which the workpiece acts as anode and the wire is the cathode (tool). The workpiece can be shaped by relative motion between it and the wire. Wire ECM is similar to wire electro-discharge machining (WEDM) in principle. WECM has advantages over the shaped tool ECM. Moreover, WECM has a great advantage over WEDM, which is the absence of heat-affected zone around the cutting area [10–14].

Maeda et al. [11] studied the effect of working parameters such as electrolyte flow rate, nozzle diameter, workpiece material, diameter and tension of wire, and the peak value, and the pulse period of the applied voltage on the maximum feed rate of cutting that can be attained by the wire without short-circuiting during WECM. They concluded that the wire feed rate that can be attained without short-circuiting increases with the increase in applied voltage, but at the same time, it is restricted by increasing of the electrolyte temperature. This increase is due to the increase of current density inside the working area, which leads to an increase in the metal removal rate; hence the maximum feed rate can be increased.

Hewidy [12] cuts electrochemically a mild steel plate with non-passivating electrolyte of NaCl and a circular wire tool. It was found that the maximum feed rate which can be achieved is about 1.25 mm/min and that the minimum side gap is much greater than 1 mm. Jain and Panedy [13] reported that the main problem in EC wire cutting is the supply system for the electrolyte, which is usually of a complex nature. They used wire electrodes with uniform rectangular cross-section uninsulated at the sides. It should be noted that Jain and Panedy [13] selected a very short machining time for few seconds; thus, the case does not resemble actual wire cutting conditions. Zhu et al. [14] developed a micro-wire electrochemical cutting process to make complex profiles. They used tungsten wire electrode with the diameter of 5 μm for producing micro-structures with a slit width <20 μm.

The ECM process provides its adequacy to cut hard material with different shapes and its applications are widely increased. However, the literature survey shows that the most problem encountered in electrochemical machining is the use of profiled tool and the lack of accuracy. Furthermore, it is clear that there is no attempt to use the wire as a tool in electrochemical turning process. The objective of this study is to investigate the use of wire in electrochemical turning process instead of using profiled tool. This method of using wire as an electrode is applied on WECGT process. The effects of important machining parameters, namely, wire diameter (d), rotational speed (N), and feed rate (f_r) on the process performance such as MRR, groove width (W), and roundness error (RE) were studied. The experimental design and results analysis were performed using a response surface methodology (RSM). Two responses, i.e., MRR and roundness error have been optimized simultaneously based on composite desirability optimization technique.

2 Experimental work

2.1 Experimental setup

The design and development of the WECGT setup is based on the problem objectives, various relevant design considerations applicable to different system elements, operational efficiency, and flexibility, as well as manufacturing and cost considerations. The proposed WECT system shown in Fig. 1 comprises major subsystems: power supply, electrolyte supply and cleaning system, WECGT tool and drives, work holding and positioning system, and frame and housing. This system consists of a numerical control laboratory mechanism with three, X, Y, and Z, axes motions. The X-axis provides the horizontal motion (parallel to the workpiece axis), while the Y-axis provides the vertical motion. The

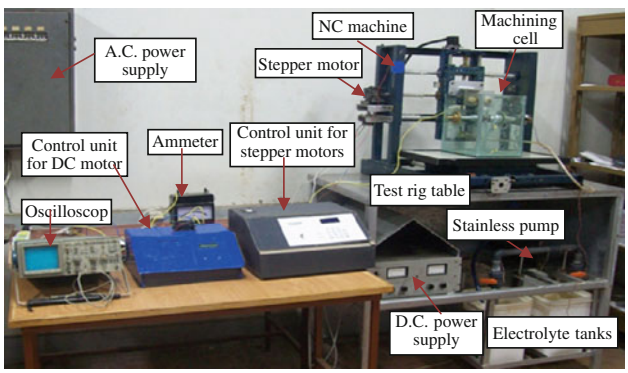

Fig. 1 Photographic view of the proposed WECT system

rotation of the workpiece is around the *X*-axis. One end of the workpiece is clamped using a rotatable chuck and the other end by a center. The chuck axis rotates on a ball bearing and connected directly to a DC motor by means of a Teflon sleeve. This sleeve is internally turned from both sides to the size of the chuck axis diameter and the other end to the DC motor axis diameter. The two axes are fixed in the sleeve using a pin key. The number of revolutions of the workpiece is the same as that of the DC motor.

The tool (wire) was fixed with a copper holder to resist corrosion. This holder was designed in a way such that it permits a nozzle to be fixed on it. One end of the wire was fixed in the nozzle a way permitting the electrolyte to be advanced from the nozzle around it. The electrolyte enters the nozzle through a side opening. The other end of the wire was fixed in a bolt used for tightening the wire. Figure 2 shows solid model of the wire holder, and Fig. 3 presents a photographic view of the wire–workpiece combination. Electrolyte was pumped using a stainless steel pump for supplying the electrolyte to the inlet nozzle around the wire.

The electric system consists of:

- DC power supply provides maximum 60 V and 50 A.
- Micro-controller (ATMEGA8535L, 8PI, 0514A) through which the speed of the motors can be controlled by a software program loaded on it.
- Driver circuit for the micro-controller to perform its function properly.

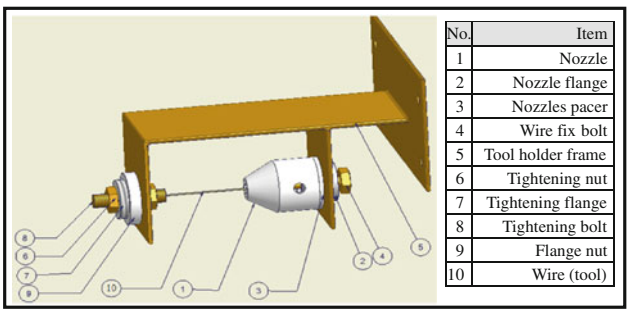

Fig. 2 Solid model for the wire holder

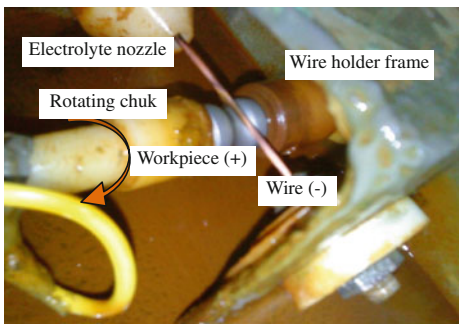

Fig. 3 Photographic view of the wire–workpiece combination

The speed of the stepper motor is controlled by the number of pulses sent to the stepper motor from the micro-controller. The program loaded on the micro-controller handles with the stepper motor in the way of half-step technique. However, there is a limit for the minimum and maximum speed of the motor. Minimum speed is the speed at which the motor rotates smoothly without stepping, and maximum speed is the speed at which the motor has the minimum torque required to rotate the axis connected to the motor. The minimum speed in the *X* and *Y*-axes is 0.01 mm $min^{-}1$. This speed is accomplished by the minimum speed of the stepper motor and a reduction system.

2.2 Experimental procedure and measurements

In this study, a commercial brass circular cross-section wire with different diameters (0.2–2.8 mm) was used as a tool. Mild steel workpieces in a shape of bars of diameter 20 mm were machined to a length of 40 mm. The length was divided equally into two portions; the first one with 14 mm diameter from which the workpiece was clamped by the chuck. The diameter of the other portion was reduced to 16 mm on which the electrochemical turning is preformed. The feed rate of the stepper motor was calibrated using a dial gauge (Mitutoye, 0:5 mm, 0.01 mm) and stop watch. The specimen was weighted before and after machining using a digital balance (Sartorius, type 1712, 0.0001 g). The specimen diameter was measured using digital micrometer (Mitutoye, 0-25 mm, 0.001 mm). The metal removal rate was specified using the following equation:

$$MRR = \frac{W_b - W_a}{t} \quad (1)$$

where W_b is the specimen weight before machining (g), W_c is the specimen weight after machining (g), and t is the machining time (min).

The roundness error of the machined workpieces was measured using a roundness tester (Mitutoye, Round Test RA-100). Each roundness error is obtained by averaging four measurements at equal positions along the axial direction of the workpiece surface for each machining condition. The groove width obtained by WECGT process was measured using digital microscope (Mitutoye, Japan, Toolmaker Microscope, 0.001).

2.3 Experimental design

The accuracy and effectiveness of an experimental program depends on careful planning and execution of the experimental procedures. With a view to achieving the aforementioned aim, in this study experiments were carried out according to a central composite second-order rotatable design based on RSM [15–20]. Response surface methodology is a collection

of mathematical and statistical techniques useful for modeling and optimizing the response variable models involving quantitative independent variables.

In this experimental study, the following independently controllable process parameters were identified to carry out the experiments: wire diameter (d), rotational speed (N), and radial feed rate (f_r). The working range was selected on the basis of data given in the literature surveys [10–14], reviews of experience, and trial experiments. Table 1 presents the constant operating conditions. The experiments are designed at three levels as shown in Table 2. Table 3 presents the experimental design matrix. The actual value of the interval between the levels is calculated from the equation:

$$\Delta Z_i = \frac{Z_i^{\max} - Z_i^{\min i}}{n-1} \tag{2}$$

$$Z_i^0 = \frac{Z_i^{\max} - Z_i^{\min i}}{2} \tag{3}$$

where $i = 1, 2, 3, \ldots, k$, ΔZ_i is the actual interval between the levels of input parameter Z_i, $Z_i^{\max}$ is the maximum value of input parameter Z_i, $Z_i^{\min i}$ is the minimum value of input parameter Z_i, Z_i^o is the center point of variable Z_i, n is the Number of levels, and k is the number of input parameters.

Table 1 Constant operating conditions

Working condition	Value
Workpiece material	Mild steel
Tool material	Brass
Electrolyte type	NaCl
Electrolyte concentration	250 g l^{-1}1
Electrolyte flow rate	15 l min^{-1}1
Electrolyte pressure	2 MPa
Applied voltage	24 V
Initial gap	0.5 mm
Machining distance	1.5 mm
Nozzle diameter	8 mm

Table 2 Coded and actual values of the input parameters

Input parameters	Symbol	Levels		
		−1	0	+1
Radial feed rate, f_r/mm min^{-1}1	X_1	0.06	0.08	0.1
Wire diameter, d/mm	X_2	1.1	2	2.8
Rotational speed, N/rpm	X_3	450	675	900

3 Mathematical modeling

Through the use of the design of experiments and applying regression analysis, the modeling of the desired response to several independent input variables can be gained. If all variables are assumed to be measurable, the response surface can be expressed as follows:

$$Y_u = f(X_1, X_2, X_3, \ldots, X_k) \pm \varepsilon \tag{4}$$

The response function representing the WECGT performance can be expressed as:

$$Y_u = b_0 + \sum_{i=1}^{n} b_i X_{iu} + \sum_{i=1}^{n} b_{ii} X_{iu}^2 + \sum_{j>i}^{n} b_{ij} X_{iu} X_{ju} + \varepsilon \tag{5}$$

where Y_u is the corresponding response, X_i (1, 2,… n) are the coded levels of n controlling machining parameters,

Table 3 Experimental design matrix and results of the output parameters

Exp. No.	Wire diameter		Radial feed rate		Rotational speed		Output parameters		
	Coded X_1	Actual/mm	Coded X_2	Actual/mm min^{-1}	Coded X_3	Actual/rpm	MRR/g min^{-1}	W/mm	RE/μm
1	1	2.8	−1	0.06	1	900	0.188	9.574	7.3
2	1	2.8	1	0.1	−1	450	0.355	9.03	21.75
3	−1	1.1	1	0.1	1	900	0.239	8.804	24.58
4	−1	1.1	−1	0.06	−1	450	0.237	9.5	28.85
5	−1	1.1	0	0.08	0	675	0.244	9.453	18.87
6	1	2.8	0	0.08	0	675	0.266	10.355	5.98
7	0	2	0	0.08	−1	450	0.371	9.618	20.52
8	0	2	0	0.08	1	900	0.268	9.618	11.77
9	0	2	−1	0.06	0	675	0.263	9.75	6.72
10	0	2	1	0.1	0	675	0.315	9.39	12.6
11	0	2	0	0.08	0	675	0.314	9.954	8.7
12	0	2	0	0.08	0	675	0.291	9.964	8.86
13	0	2	0	0.08	0	675	0.302	9.726	8.92
14	0	2	0	0.08	0	675	0.31	9.912	8.69
15	0	2	0	0.08	0	675	0.3	9.986	8.8

and ε is the experimental error. The terms b_0, b_1, etc. are the second-order regression coefficients. The second term under the summation sign of this polynomial equation is attributable to the linear effect, whereas the third term corresponds to the higher-order effects. The fourth term of the equation includes the interactive effects of the process parameters. Applying the least square technique, the values of these coefficients can be estimated using the collected (Y_1, Y_2,...Y_k) through the design points k [15–17]. Using the collected results shown in Table 3, the final mathematical models for MRR, groove width (W), and roundness error (RE) as determined by the preceding analysis are:

$$MRR = -0.30452 + 0.38351\,d + 9.3371\,f_r - 3.75733 * 10^{-4}\,N - 0.60294\,d f_r - 1.23938 * 10^{-3}\,f_r N - 0.067892\,d^2 - 37.65488\,f_r^2 \quad (6)$$

$$W = 6.8257 - 1.33384 * 10^{-4} d + 71.89992 f_r + 6.79739 * 10^{-4}\,dN + 0.083337 f_r N - 884.4430 f_r^2 \quad (7)$$

$$RE = 124.61232 - 29.84768\,d - 171.04711\,f_r - 0.2126\,N + 17.94118\,d f_r + 2.06536 * 10^{-3}\,dN - 0.076414\,f_r N + 4.98542\,d^2 + 2091.50929\,f_r^2 \quad (8)$$

Table 4 ANOVA for MRR

Source model	DF	SS	MS	*F*-value	*P*-value
	9	0.031528	0.003503	54.93807	0.0002
d	1	0.00025	0.00025	3.921266	0.1045[a]
f_r	1	0.001352	0.001352	21.20323	0.0058
N	1	0.005305	0.005305	83.18973	0.0003
$f_r\,d$	1	0.00014	0.00014	2.196907	0.1984[a]
$d\,N$	1	0.000352	0.000352	5.521674	0.0656
$f_r\,N$	1	4.15E-05	4.15E-05	0.651074	0.4564[a]
d^2	1	0.00629	0.00629	98.64813	0.0002
f_r^2	1	0.000593	0.000593	9.30617	0.0284
N^2	1	0.000623	0.000623	9.776724	0.0261
Residual	4	0.000319	6.38E-05		
Lack of fit	2	5.01E-05	2.5E-05	0.279457	0.7739[a]
Pure error	2	0.000269	8.96E-05		
Core total	13	0.031846			

DF degree of freedom, *SS* sum of squares, *MS* mean of squares

[a] Non-significant term

Table 5 ANOVA for groove width

Source model	DF	SS	MS	*F*- value	*P*-value
	9	2.074546	0.230505	24.95246	0.0012
d	1	0.405631	0.405631	43.91001	0.0012
f_r	1	0.0648	0.0648	7.014679	0.0455
N	1	0	0	0	1.0000[a]
$f_r\,d$	1	0.001925	0.001925	0.20842	0.6672[a]
dN	1	0.022533	0.022533	2.439261	0.1791[a]
f_rN	1	0.187701	0.187701	20.31885	0.0064
d^2	1	0.001048	0.001048	0.113466	0.7499[a]
f_r^2	1	0.327373	0.327373	35.43854	0.0019
N^2	1	0.244565	0.244565	26.47441	0.0036
Residual	4	0.046189	0.009238		
Lack of fit	2	0.00173	0.000865	0.058363	0.9444[a]
Pure error	2	0.044459	0.01482		
Core total	13	2.120735			

Table 6 ANOVA for roundness error

Source model	DF	SS	MS	*F*-value	*P*-value
	9	760.0141	84.44601	5467.652	<0.0001
d	1	83.04177	83.04177	5376.731	<0.0001
f_r	1	17.2872	17.2872	1119.3	<0.0001
N	1	38.28125	38.28125	2478.608	<0.0001
$f_r\,d$	1	0.124033	0.124033	8.030825	0.0365
$d\,N$	1	0.208033	0.208033	13.4696	0.0144
$f_r\,N$	1	0.157814	0.157814	10.21802	0.0241
d^2	1	33.9182	33.9182	2196.112	<0.0001
f_r^2	1	1.830724	1.830724	118.5344	0.0001
N^2	1	140.2154	140.2154	9078.57	<0.0001
Residual	4	0.077223	0.015445		
Lack of fit	2	0.050823	0.025412	2.887686	0.1999[a]
Pure error	2	0.0264	0.0088		
Core total	13	760.0913			

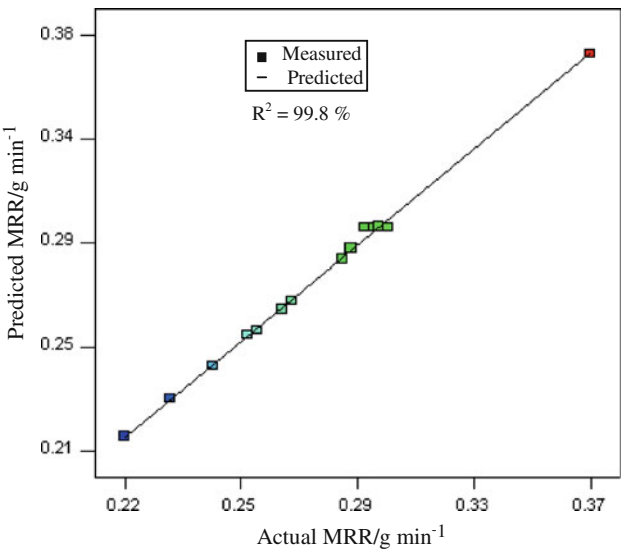

Fig. 4 Predicted versus measured values for MRR

It should be noted from the final equations that there are some coefficients omitted. These coefficients are non-significant according to a Student's t test. The adequacies of the models developed for the responses Y_u are checked using the analysis of variance technique. Through this technique, the F-ratio for each term in the developed model is determined to know the significant and non-significant terms. Furthermore, the lake of fit of each model is determined to measure the deviation of the response from the fitted surface. Design Expert software (version 7.0.0, State Ease Inc. Minneapolis) was used to analyze the experimental data of the response parameters. From Tables 4, 5, and 6, it is evident that the models are adequate. The scatter diagrams depicted in Figs. 4, 5, and 6 clearly show that the predictions made by the mathematical models are in good agreement with the experimental results value.

4 Results and discussion

Based on RSM, the developed mathematical models (Eqs. 6–8) can be employed to predict the WECGT performance for the range of process parameters used in this investigation by substituting their respective values in actual form. Based on these models, the main and the interaction effect of process parameters on MRR, groove width, and roundness error were computed and plotted in Figs. 7, 8, 9, 10, 11, 12, 15, 16, 17, and 18.

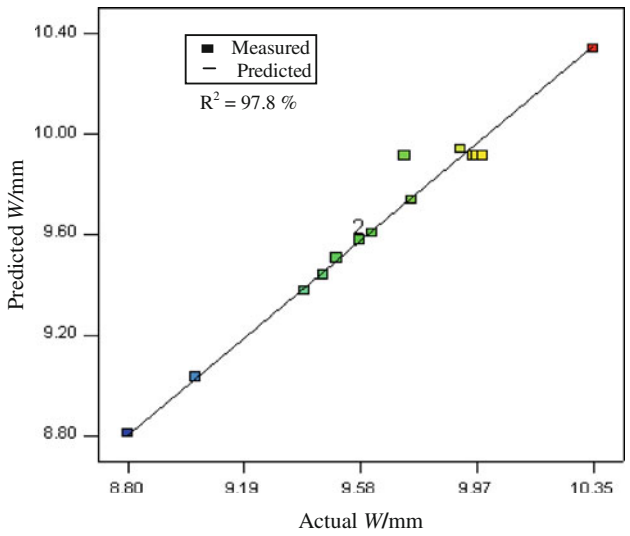

Fig. 5 Predicted versus measured values for groove width

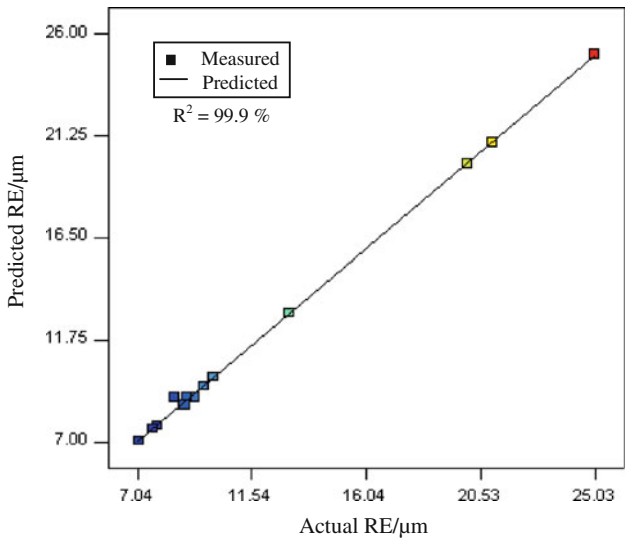

Fig. 6 Predicted versus measured values for roundness error

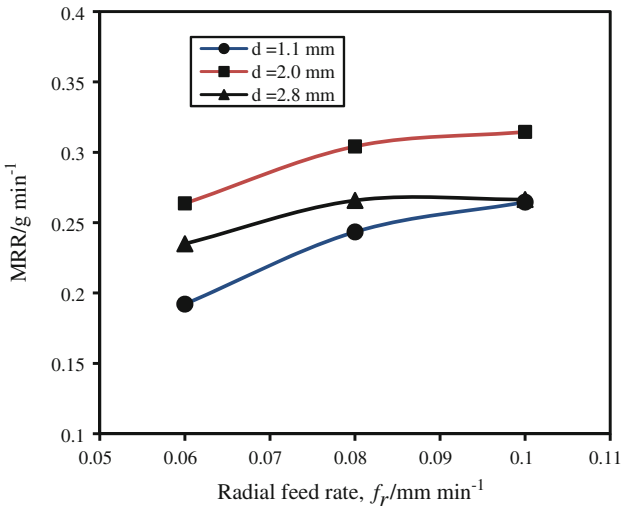

Fig. 7 Effect of radial feed rate on MRR at various wire diameters ($N = 675$ rpm)

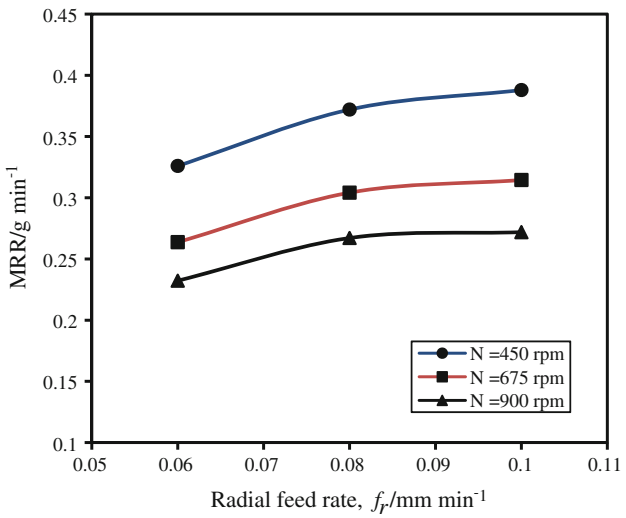

Fig. 8 Effect of radial feed rate on MRR at various rotational speeds ($d = 2$ mm)

4.1 Effects of machining parameters on metal removal rate

Figures 7 and 8 show the effect of radial feed rate on the metal removal rate at various values of wire diameter and rotational speed. Non-linear relationship between radial feed and MRR is observed. It is noted that the MRR increases with increasing the radial feed up to 0.08 mm min^{-}1 afterward MRR decreases. This result is attributed to the increase of the current density with the increase of radial feed rate. At low feed rates, the metal removal is reasonable and does not affect the inter-electrode gap resistance. On the other hand, at high feed rates, the martial removal is large and may accumulate. The latter effect increases the gap resistance, and hence, decreases the current density which, in turn, decreases the MRR.

The effect of wire diameter on the MRR at various values of rotational speed is shown in Fig. 9. It is observed that the MRR increases with the increase of wire diameter up to a certain value (2 mm) and afterward, the MRR decreases. This result may be attributed to the exit area of the nozzle available for the electrolyte. At small wire diameters there is large exit area which provides large number of electrolytic ions in the machining gap. At large wire diameters, the wire takes large area from the nozzle area and hence the provided number of electrolytic ions from the nozzle exit is small. In addition, when the available exit area is small, the electrolyte is advanced at higher velocity compared to large exit area. This may lead to electrolyte disturbance, and hence, possibility of entering air into the machining gap. Thus, the electrical resistance of the electrolyte increases.

Based on RSM model (Eq. 6), the influence of the rotational speed on the MRR at various values of feed rate and wire diameter is illustrated in Figs. 8 and 9. It is clear that the rotational speed significantly affects the MRR (see Table 4). The MRR increases with the decrease in the rotational speed. This is due to the separation of the electrolyte outward from the circumference of the workpiece surface at high rotational speed which decreases the MRR.

4.2 Effects of machining parameters on groove width

Figures 10 and 11 exhibit the effect of radial feed rate on the groove width at different values of wire diameter and rotational speed. In general, the groove width decreases with the increase of radial feed rate. This is because the time available for the stray current effect to cut from the sides of the groove decreases with the increase in the feed rate. This leads to produce small groove width.

Figures 10 and 12 demonstrate the effect of the wire diameter on the groove width at various values of feed rate and rotational speed. It is noted that the groove width increases with the increase in the wire diameter. This result is attributed to the increase in the width of the machining area with the increase in the wire diameter. In addition, the stray current effect increases when using large wire diameter due to the increase in the wire side area (see Fig. 13). This in turn increases the groove width. Figure 14a, b shows the main features of two different grooves produces at maximum and minimum wire diameters. Figure 14 and Table 5 show that the wire diameter has a great influence on the groove width value.

The effect of rotational speed on the groove width at various values of radial feed rate and wire diameter is shown in Figs. 11 and 12. It is observed that an increase in the rotational speed leads to a decrease in the groove width. This effect may be due to the electrolyte hydrodynamic

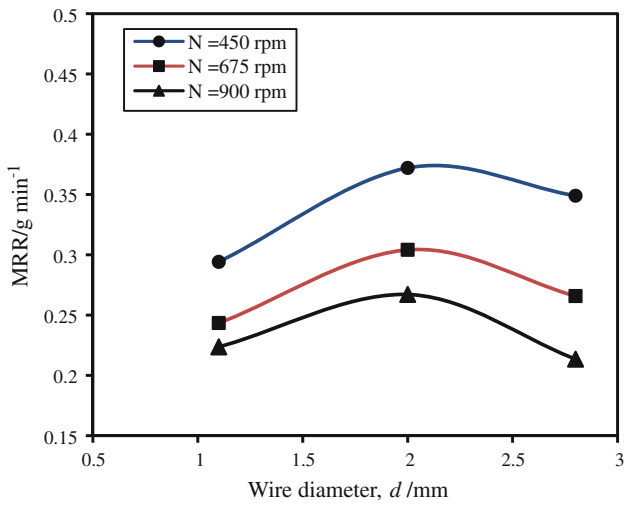

Fig. 9 Effect of wire diameter on MRR at various rotational speeds (fr = 0.08 mm min^{-}1)

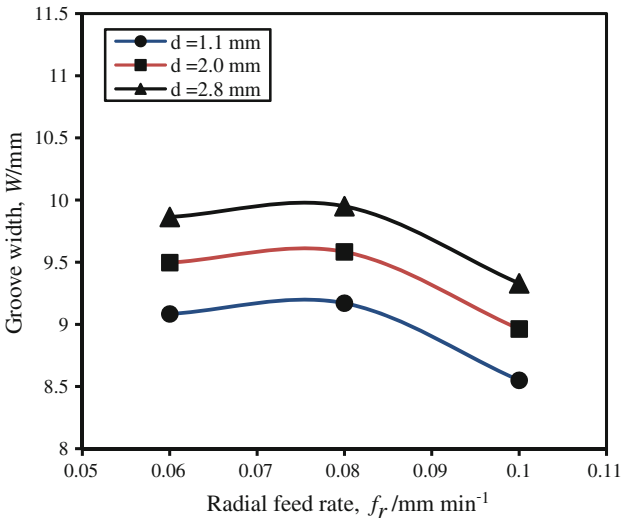

Fig. 10 Effect of radial feed rate on groove width at various wire diameters (N = 675 rpm)

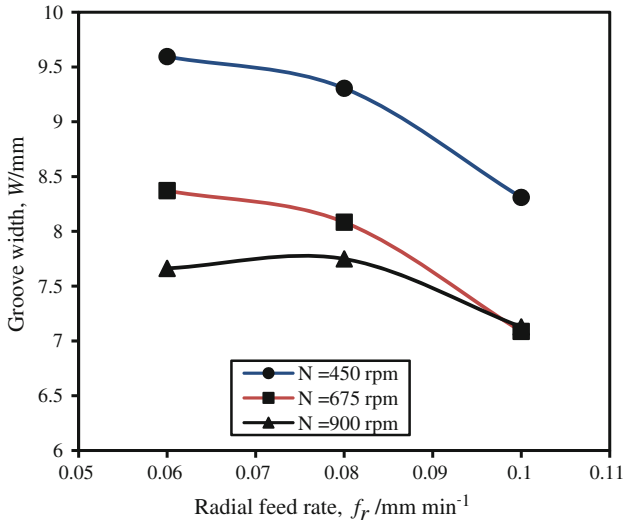

Fig. 11 Effect of radial feed rate on groove width at various rotational speeds ($d = 2$ mm)

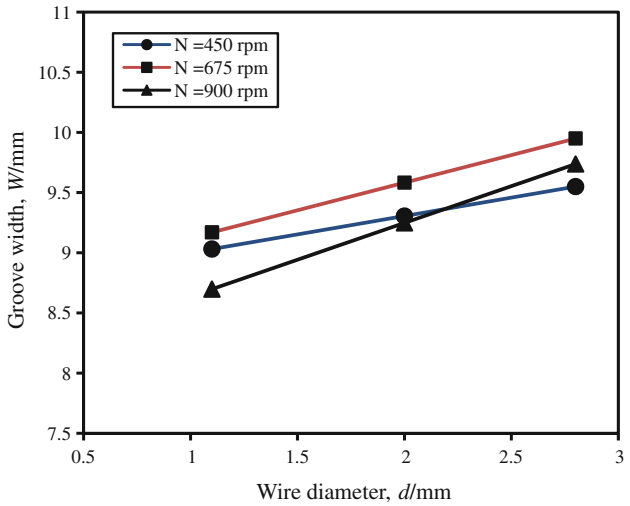

Fig. 12 Effect of wire diameter on groove width at various rotational speeds ($fr = 0.08$ mm min^{-}1)

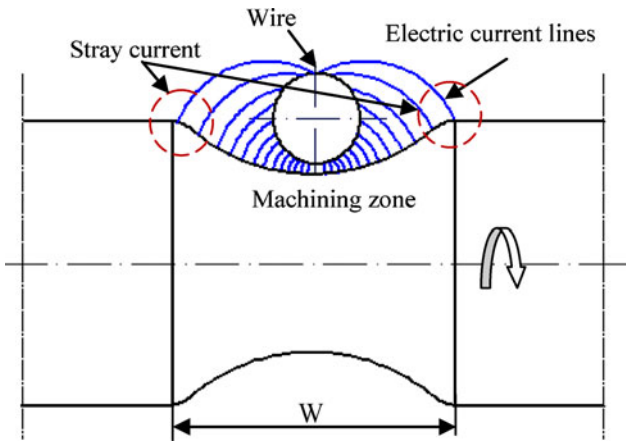

Fig. 13 Stray current effect on groove width

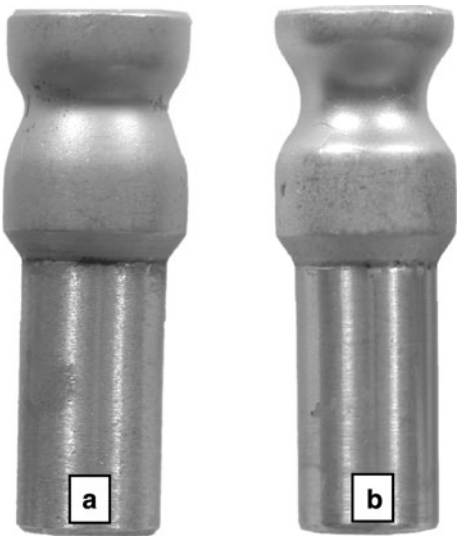

Fig. 14 Groove width comparison at: (**a**) $d = 1.1$ mm, $fr = 0.08$ mm min^{-}1, $N = 675$ rpm (**b**) $d = 2.8$ mm, $fr = 0.08$ mm min^{-}1, $N = 675$ rpm

instability over the workpiece surface during its rotation. This leads to decreasing the effect of the stray currents on the groove width.

4.3 Effects of machining parameters on roundness error

Roundness errors are considered as one of the important geometrical errors of axis-symmetric parts because they have negative effects on the accuracy and other important factors such as the fitting machine elements and wear in rotating elements. Based on a non-linear mathematical model of RE through RSM, Figs. 15 and 16 show the effect of radial feed rate on the roundness error at various values of wire diameter and rotational speed. It is noted that the roundness error slightly increases with the increase of radial feed rate. This result is due to the increase of metal removal rate with the increase of feed rate. Any increase in radial feed rate increases the current density in the gap between wire and workpiece surface which enhances the anodic dissolution of the work material. This results in higher material removal rate and produces with larger roundness error. The deterioration in the roundness error may be attributed partly to stray current effects. This result is in agreement with that obtained previously [5, 19]. Figure 17a, b illustrates a comparison of roundness error profiles of two samples machined by WECGT process at maximum and minimum value of radial feed rates. It should be noted that the increasing of radial feed rate value from 0.06 mm/min to 1 mm/min increases the roundness error twice.

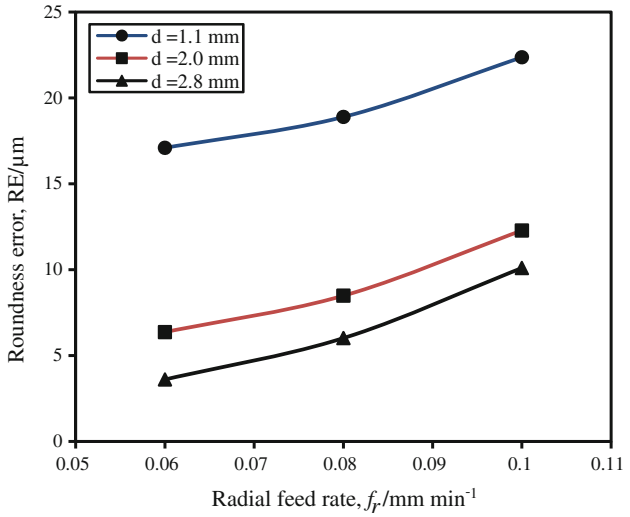

Fig. 15 Effect of feed rate on roundness error at various wire diameters ($N = 675$ rpm)

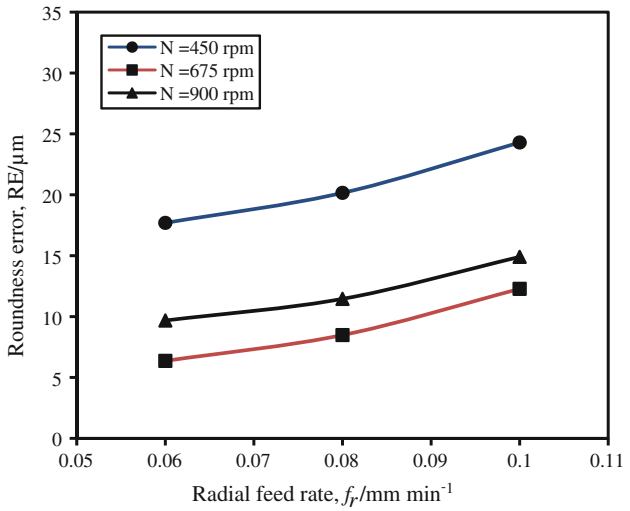

Fig. 16 Effect of radial feed rate on roundness error at various rotational speeds ($d = 2$ mm)

Figures 15 and 18 show the effect of wire diameter on the roundness error at various values of radial feed rate and rotational speed. It is observed that the roundness error decreases dramatically with the increase of the wire diameter up to 2 mm; afterward, the wire diameter has small effect on the roundness error. This may be attributed to the increase of the machining area with the increase in the wire diameter. Furthermore, Table 6 proves that the wire diameter plays the important role on resultant roundness error.

The effect of the rotational speed on the roundness error is shown in Figs. 16 and 18 at various values of radial feed rate and rotational speed. It is noted that the roundness error is improved with the increase in rotational speed. This can be explained by the nature of the WECGT process. When the rotational speed is high, smaller thickness is removed per revolution. When the process stops, a step height will remain in the place where the electrode happens to be at the moment [21, 22]. However, this step is spread over the width of the wire which is exposed to the machining.

5 Optimal results

The objective of using RSM is not only to investigate the response over the entire factor space, but also to locate the region of interest where the response reaches its optimum or near optimal value. Derringer and Suich [23] describes a multiple response method called desirability. It is an attractive method for industry for optimization of multiple quality characteristic problems. The method makes use of an objective function, $D(X)$, called the desirability function (utility transfer function) and transforms an estimated response into a scale free value called desirability. The desirable ranges are from zero to one (least to most desirable, respectively). One represents the ideal case; zero

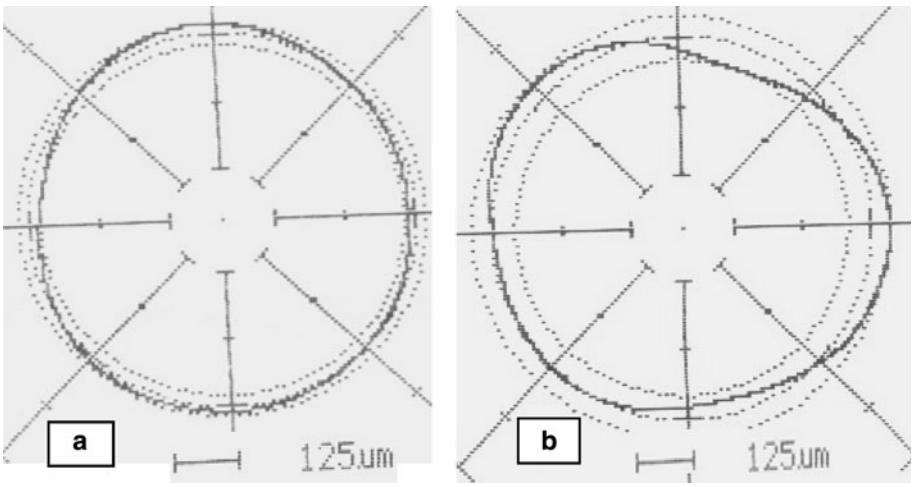

Fig. 17 Comparison of roundness error profile at: (**a**) $f_r = 0.1$ mm min^{-1}, $d = 2.8$ mm, $N = 675$ rpm (**b**) $f_r = 0.06$ mm min^{-1}, $d = 2.8$ mm, $N = 675$ rpm

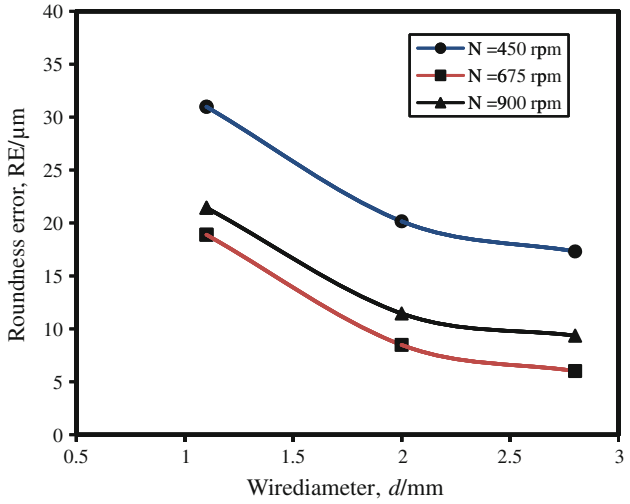

Fig. 18 Effect of wire diameter on roundness error at various rotational speeds ($fr = 0.08$ mm min^{-}1)

indicates that one or more responses are outside their acceptable limits. Composite desirability is the weighted geometric mean of the individual desirabilities for the responses. The factor settings with maximum total desirability are considered to be the optimal parameter conditions. The simultaneous objective function is a geometric mean of all transformed responses [24, 25]. Two responses, i.e., MRR and RE have been optimized simultaneously using developed models, i.e., Eqs. 6 and 8 based on composite desirability optimization technique. In response optimization, a measure of how the solution has satisfied the combined goals for all responses must be assured. The optimality solution is to evaluate the input parameters in experiment range for maximizing MRR and minimizing RE. The numeric values of optimum conditions and the predicted optimum values of responses under these conditions are presented in Tables 7 and 8.

Table 7 Constrains of input parameters and optimum values

Parameter	Goal	Optimum value
Radial feed rate, f_r/mm min^{-}1	In range	0.08
Wire diameter, d/mm	In range	2.3
Rotational speed, N/rpm	In range	587

Table 8 Predicted optimum values of responses

Response	Goal	Predicted
MRR/g min^{-}1	Maximize	0.325
Roundness error, RE/μm	Minimize	9.573

6 Conclusions

Based on the results and discussion presented in the preceding section, the following conclusions have been drawn:

1. The response surface methodology used in this study proves its adequacy to be an effective tool for investigating the process parameters with a number of experiments reached 2.5% of the tests required by the classical method.
2. Using wire as an electrode in electrochemical turning instead of using a profiled tool proved its power to produce circular grooves.
3. The groove width in WECGT process has greatly increased by increasing the wire diameter, while it is decreased by increasing both the radial feed rate and the rotational speed.
4. Lower roundness errors are obtained by increasing both radial feed rate and wire diameter.
5. Using the high rotational speed improves roundness error whereas it reduces the process productivity.
6. The optimum combination of parameters setting is: radial feed rate of 0.08 mm min^{-}1, wire diameter of 2.3 mm, and rotational speed of 587 rpm for maximizing MRR and minimizing roundness error.

Finally, future research can be devoted toward investigating the effect of other parameters on the process performance such as nozzle diameter, using of different geometries of wire cross-section, using pulsed voltage instead of DC voltage, and using different inclinations of the wire.

Acknowledgments The authors acknowledge the workshop staff members of High Institute of Technology, Benha University, Benha, Egypt for their help in the carrying out the experimental setup of this study.

References

1. Derringer G, Suich R (1980) Simultaneous optimization of several response variables. Jof Qual. Technol 12:214–219
2. Weller EJ, Mtthew Haavisto (1984) Non-traditional machining processes. Society of Manufacturing Engineers, DearBorn, Michigan
3. Castillo ED, Montgomery DC, McCarville DR (1996) Modified desirability functions for multiple response optimization. J Qual Technol 28:337–345
4. El-Taweel TA (2008) Modelling and analysis of hybrid electrochemical turning-magnetic abrasive finishing of 6061 Al-Al_2O_3. Int J Adv Manuf Technol (IJAMT) 37:705–714
5. Munda J, Bhattacharyya B (2008) Investigation into electrochemical micromachining (EMM) through response surface methodology based approach. Int J Adv Manuf Technol 35: 821–832
6. Montgomery DC (2001) Design and analysis of experiments. Wiley, New York
7. Hofstede A, Van Den Brekel JW (1970) Some remarks on electrochemical turning. Annals of the CIRP XVIII:93–106

8. Hewidy MS (1982) Electrochemical wire cutting, PhD thesis, Shebin El Kom, Faculty of Engineering, Mumifia University, Egypt
9. Ebeid SJ, El-Taweel TA (2005) Surface improvement through hybridization of electrochemical turning and roller burnishing based on the Taguchi technique, Proceeding of the Institution of Mechanical Engineers, part B: J Eng Manuf 219:423–430
10. Ebeid SJ, Hewidy MS, El-Taweel TA, Youssef AH (2004) Towards higher accuracy for ECM hybridized with low frequency vibrations using the response surface methodology technique. J Mater Process Technol 149:428–434
11. Jain VK, Pandey PC (1979) An analysis of electrochemical wire cutting process using finite element technique, Proceeding of 20th MTDR Conference: 631–636
12. Antony J (2003) Design of experiments for engineers and scientists, Linacre House, Jordan Hill, Oxford OX2 8DP
13. Zhu D, Wang K, Qu NS (2007) Micro wire electrochemical cutting by using in situ fabricated wire electrode. Annals of the CIRP 56:241–244
14. El-Taweel TA (2009) Multi-response optimization of EDM with Al-Cu-Si-TiC P/M composite electrode. Int J Adv Manuf Technol 44(1/2):100–113
15. El-Taweel TA, Ebeid SJ (2009) Effect of hybrid electrochemical smoothing–roller burnishing process parameters on roundness error and micro-hardness. Int J Adv Manuf Technol 42:643–655
16. Shan HS (2006) Advanced manufacturing methods. Tata McGraw-Hill, New Delhi, India
17. Ghabrial SR, Ebeid SJ, Serag SM, Ayad MM (1992) A mathematical modeling for electrochemical turning, PEDAC 5th International Conference: 449–459
18. El-Taweel TA, Ebeid SJ (2007) Improvement of roundness of cylindrical parts using hybrid electrochemical smoothing and roller burnishing process, 35th MATDOR conference, Taipei, Taiwan: 85–88
19. Hocheng H, Pa PS (2003) Electropolishing of cylindrical workpiece of tool materials using disc-form electrodes. J Mater Process Technol 142:203–212
20. Maeda R, Chikamori K, Yamamoto H (1984) Feed rate of wire electrochemical machining using pulsed current. J Precis Eng 6(4):193–199
21. Bejar MA, Eterovich F (1995) Wire-electrochemical cutting with a $NaNO_3$ electrolyte. J Mater Process Technol 55:417–420
22. Dietz H, Gonther KG, Otto K, Stark G (1979) Electrochemical turning, considerations on machining rates which can be attained. Annals of the CIRP 28:93–97
23. McGeough JA (1974) Principles of electrochemical machining. Chapman and Hall, London
24. McGeough JA (1988) Advanced methods of machining, London. Chapman and Hall, New York
25. Pa PS (2008) Design of borer-rib type electrode in electrochemical smoothing of large holes. JMEPEG 17:37–43